Geofísica Internacional (2004), Vol. 43, Num. 1, pp. 75-82

Characteristics of coronal mass ejections in the near Sun interplanetary space

Alejandro Lara[1], J. Américo González-Esparza[1] and Nat Gopalswamy[2]
[1] *Instituto de Geofísica, UNAM, México D.F., México*
[2] *NASA/GSFC, Greenbelt, MD, USA*

Received: March 31, 2002; accepted: July 15, 2002

RESUMEN

Con base en las observaciones del Coronógrafo Espectrométrico de Gran Angular (LASCO) que se encuentra a bordo del Observatorio Solar y Heliosférico (SOHO) estudiamos algunos parámetros de las Eyecciones de Masa Coronal (CME) a distancias de 6 a 10 radios solares. Desarrollamos un método nuevo para calcular la duración, el incremento del brillo (sobre el nivel de fondo) y la velocidad de la estructura delantera de las eyecciones. Estas propiedades son importantes para entender la dinámica de las eyecciones cerca del Sol y son también críticas para estudiar su evolución en el medio interplanetario usando modelos numéricos. En este trabajo presentamos el método de análisis y los resultados de la aplicación de este método a un grupo de 9 eyecciones tipo halo observadas durante 1997. Encontramos que i) la velocidad de las eyecciones obtenida con este método coincide con las mediciones de otros observadores ii) la duración promedio de la parte delantera de las eyecciones es de 8 hrs, y iii) la brillantez máxima decrece con la distancia como una ley de potencias con índice promedio de -3.6.

PALABRAS CLAVE: Eyecciones de Masa Coronal, actividad solar.

ABSTRACT

Based on the observations from the Large Angle and Spectrometric Coronagraph (LASCO) on board the Solar and Heliospheric Observatory (SOHO) spacecraft we studied coronal mass ejections (CME) parameters between 6 and 10 solar radii from the Sun. We have developed a new method to obtain the duration, brightness enhancement (above the background) and speed of the leading part of the CMEs. These properties are important in order to understand the dynamics of the CMEs near the Sun and their evolution in the interplanetary space using numerical models. We present the method of analysis and the results of the application of this method to a set of 9 halo CMEs observed during 1997. We found that i) the CME speeds obtained with this method are in good agreement with measurements of other observers, ii) the average time duration of the CME leading part is 8 hrs. and iii) the brightness maxima decrease with distance as a power law with a mean index of -3.6.

KEY WORDS: Coronal Mass Ejections, solar activity.

1. INTRODUCTION

Coronal mass ejections (CME) are solar phenomena that can affect Earth's magnetospheric environment and some technological systems (see e.g. Webb *et al.*, 2000; Gopalswamy *et al.*, 2001a). The strongest geomagnetic disturbances are caused by CMEs traveling towards Earth (Vennerstroem, 2001). In order to mitigate the effects due to CME impact, we need to understand their behavior in the interplanetary medium. Recently Gopalswamy *et al.* (2000; 2001) developed an empirical model of CME acceleration using the initial speed near the Sun and the interplanetary CME (ICME) speed at 1 AU as input parameters. González-Esparza *et al.* (2002) performed one dimensional hydrodynamic simulations of CME-like disturbances to study their evolution in the interplanetary medium, reporting the strong influence that the CME parameters have on their evolution. When a CME is initiated it begins to interact with the ambient solar wind implying a strong and complex interchange of momentum. The evolution of the CME in the interplanetary medium depends on the characteristics of the CME and the ambient solar wind ahead.

A general problem in any numerical study are the initial conditions. In order to study the evolution of a CME in the interplanetary medium it is necessary to know their characteristics (density, time duration, speed, etc.) and those of the ambient solar wind near the Sun. Traditionally, the initial conditions have been assumed and adjusted semi-arbitrarily in order to obtain the best results as the output of the numerical code.

In this work we present a method to infer some CME parameters near the Sun such as the time duration, speed and brightness enhancement (as an approximation to the CME density), at heliocentric distances of 6 to 10 solar radii (R_s)

where CMEs are well observed by the Large Angle and Spectrometric Coronograph (LASCO) on board the Solar and Heliospheric Observatory (SOHO). These physical properties can be used for theoretical, empirical and numerical models of CMEs.

In section 2 we describe the data and the method of analysis used in this work. Next, we deduce and discuss the time duration of each event (section 3). The brightness increase during the CME at different radial distances is described in section 4. In section 5 we obtain the CME speed as deduced from the movement of both: the brightness peak and the outer edge of the CME. We discuss briefly the limitations of the method in section 6 and finally present our conclusions in section 7.

2. DATA AND METHODOLOGY

2.1 Data

We used white light images from the LASCO C3 telescope on board the SOHO spacecraft. LASCO C3 images the outer corona from ~ 5 to ~ 30 R_s (Bruckner *et al.*, 1995).

For this study we selected 9 halo CMEs that occurred during 1997. These CMEs were semi-arbitrarily selected based in the data coverage of each event. As an example, we have shown the August 30, 1997 CME in Figure 1. This CME originated from close to the disk center (N29E15) with a slight north-easterly bias. The CME was first seen in the field of view of the C2 coronograph at 01: 30 UT. All figures throughout this paper refer to this halo CME.

2.2 Methodology

In order to infer the approximated CME properties, we used the following procedure:

1. Obtain and calibrate the LASCO C3 images near and after the CME onset time.

2. Select a position angle (PA, measured from Solar North counter-clockwise) where the CME brightness enhancement is better observed (the continuous line marked as "CPA" in Figure 1). With one exception, we used the same CPA as identified in the LASCO CME catalog (http: // cdaw.gsfc.nasa.gov, Yashiro *et al.*, 2003, manuscript under preparation). This will help us to compare our measurements with those documented in the CME catalog for consistency.

3. Compute the coronal brightness at several heliocentric distances, R = 6, 7,...,15 R_s in eleven PA directions sepa-

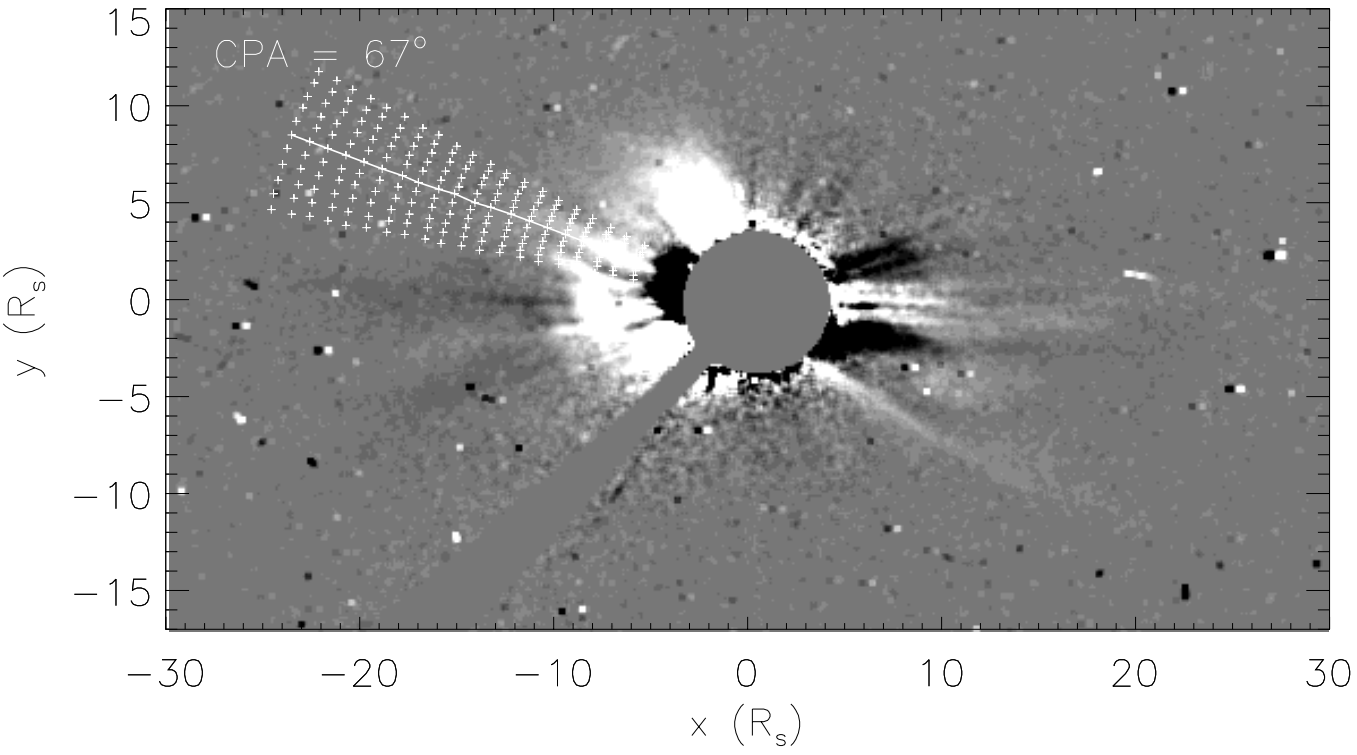

Fig. 1. A LASCO C3 difference image of the August 30, 1997 CME. The continuous line shows the central position angle (CPA) at which the CME parameters are measured. The plus symbols mark the positions where the brightness is measured for further analysis. The inner gray circle represents the occulting disk of LASCO C3. The bright feature surrounding the occulting disk in the halo CME in question.

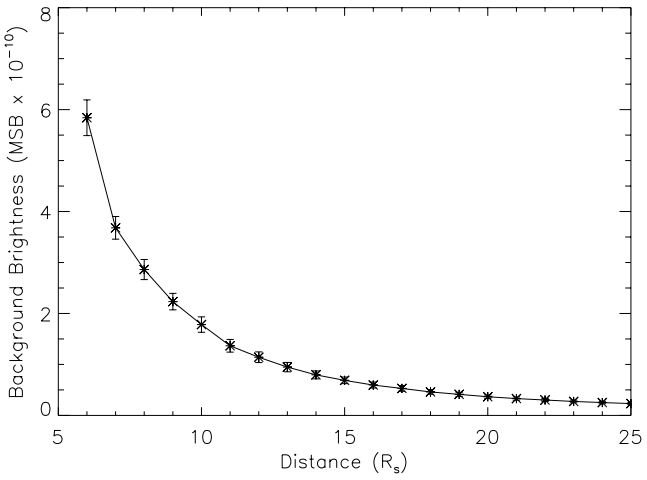

Fig. 2. Mean background brightness in mean solar brightness (MSB) units in LASCO C3 images as computed from 6 to 25 R_s.

rated by ~ 2° centered around CPA (marked with plus symbols in Figure 1). In order to avoid noise fluctuations and to perform a simple error analysis, we obtain the mean and variance (or standard deviation) of the brightness in the eleven PA directions at each selected R. This is equivalent to measuring the mean brightness in a cone of 20° wide around the CPA as a function of the heliocentric distance. In Figure 2 we have plotted the mean value of the background brightness and the associated error (standard deviation) as a function of the radial distance.

4. For each event, the previous steps were performed for each available image. This way, we obtain an array of brightness as a function of time and distance.

5. When we plotted the brightness versus time, the CMEs are observed as brightness enhancements (upper panel in Figure 3). In order to systematize the analysis, we fit a gaussian curve to the brightness enhancement and get the CME properties as the gaussian parameters (Gopalswamy *et al.*, 1996). In the next sections we describe these parameters. The lower panel of Figure 3 shows the gaussians fitted to the observed brightness enhancement. In both panels the higher curves correspond to smaller heliocentric distances (6 to 15 R_s).

3. TIME DURATION

We assume that the time duration (TD) of the CME leading edge is the width at half maximum of the fitted gaussian. This is a good approximation when the CME is well observed, mainly at low altitudes, from 6 to ~ 10 R_s. After this altitude the brightness enhancement could be near the noise level and the fitted gaussian can include noise enhancements.

Figure 4 shows the CME TD as a function of radial distances for the example CME. In general, the TD behavior with the distance does not show a constant trend, but changes from increasing to decreasing phases in the observed range of heights. For example the TD of the 08-30-97 CME (Figure 4) was increasing from 6 to 10 R_s, decreasing from 10 to 12 R_s, and finally showed a less pronounced increasing phase until 15 R_s.

Table 1 shows the TD for the 9 CMEs selected for our study (column 1). We have tabulated the CME TD only from 6 to 10 R_s because after this distance the brightness enhancement may be contaminated by noise fluctuations (However, the general trend was computed in the entire 6 - 15 R_s range as shown by the straight line in Figure 4). Due to lack of data we were unable to compute the brightness enhancement at 6 R_s for the 12-26-97 CME.

It is important to note that this TD corresponds to the CME leading edge and in some cases the brightness enhancement is complex and contains more than one peak. The TDs do not show any regular behavior. Table 1 shows the measured TD from 6 to 10 R_s (columns 2 to 6) for each CME. The mean TD of each event in the 6 to 10 R_s interval (column 7) is in the range 4.89 to 12.60 hrs. The rate of change of TD with distance (in hrs/R_s) computed over 6 - 15 R_s is

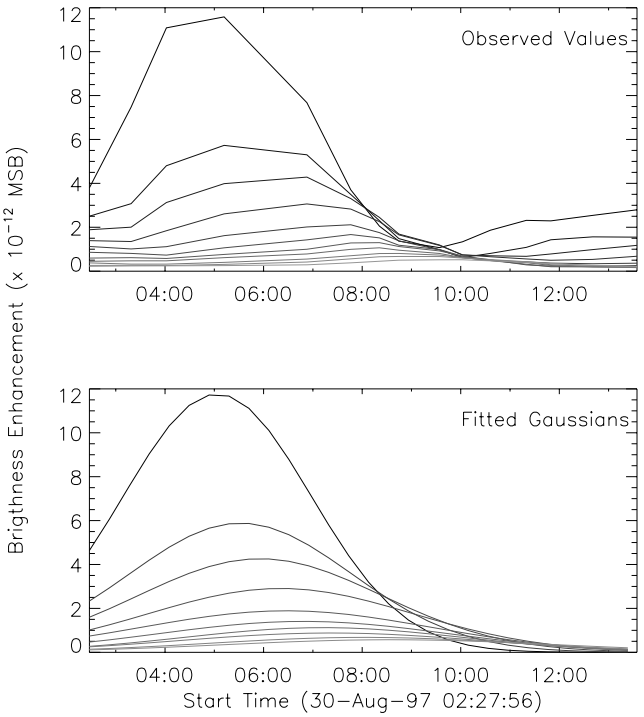

Fig. 3. CME brightness enhancement as a function of time. From top to bottom, each curve represents the brightness change at 6, 7, ..., 15 R_s. The observed values are plotted in the top panel and the respective fitted gaussians are in the bottom panel.

Table 1

CME Time Duration

date	6	7	8	9	10	mean	rate
			hrs.				hrs/R_s
02-07-97	7.76	8.71	9.37	8.16	7.55	8.31	-0.07
04-07-97	4.60	5.21	4.64	5.34	5.81	5.12	0.19
04-16-97	10.38	9.75	9.99	9.89	9.29	9.86	-0.20
05-12-97	9.55	9.17	9.89	10.15	10.29	9.81	0.38
08-30-97	3.80	4.51	4.94	5.36	5.84	4.89	0.31
09-17-97	11.12	12.07	12.01	13.48	14.32	12.60	0.75
09-28-97	5.69	4.58	5.77	5.54	6.20	5.56	0.16
12-06-97	7.34	7.66	7.33	6.98	4.99	6.86	-0.45
12-26-97		7.74	8.13	8.67	10.22	8.69	0.38

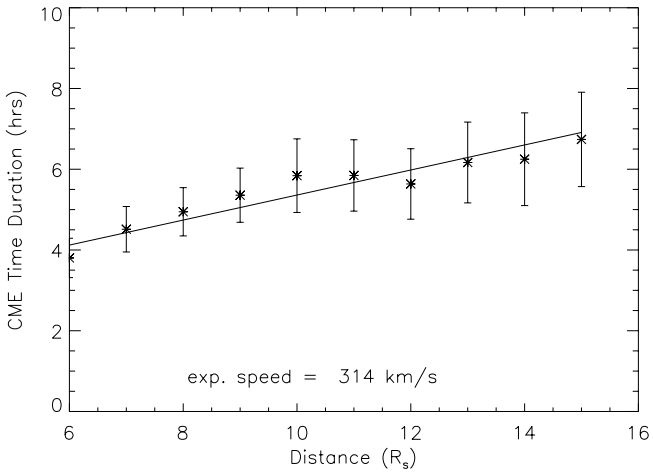

Fig. 4. Time duration of the CME leading edge as a function of heliocentric distance. A straight-line fit to the time durations corresponds to a radial expansion speed of ~314 km/s.

also tabulated (column 8). As shown in Figure 4, the TD seems to increase or decrease arbitrarily in the observed range of heights. This behavior could be caused by the lack of time coverage in the observations or by a complex interaction of the CMEs with the ambient coronal material. The general rate of change ranges from -0.45 to 0.75 hrs per R_s. This means that the maximum contraction (expansion) in the radial direction is about 0.5 (0.75) hour per solar radii.

4. BRIGHTNESS ENHANCEMENT

The CME density is hard to measure from the available data due mainly to the following reasons:

1. The contribution of different coronal species to the observed brightness: At lower altitudes, below ~ 1.3 R_s, the major contribution comes mainly from the electronic coronal component, the so called K-corona (Guhathakurta, 1989). After this distance, the contribution of the dust (F-corona) to the observed brightness becomes increasingly important until ~ 5 R_s, where it completely dominates. However, during the CME enhancement the measured brightness is due to scatering from the CME material and the dust contribution to this enhancement is negligible.

2. The inversion method to obtain the electron density using the observed polarization brightness (Van de Hulst, 1950) is fully applicable when the Sun - electron - observer (elongation) angle is ~ 90°. This means that this method is well suited for limb CMEs. For non limb-CME events the application of this method is limited and is worst when the CME direction is towards the Earth (all of our CMEs are Earth - directed).

3. The coronographs measure the brightness integrated along the line of sight. Therefore, it is difficult to obtain a good measure of the background brightness in the site where the CME takes place.

In this work we obtain the brightness enhancement (BE) corresponding to the passage of the CME at various heights from 6 to 15 R_s. In Figure 5 we have plotted the BE peak (the gaussian height) as a function of the distance. A power law of the form of $BE = c_0 R^{\alpha}$ seems to represent very well the decrease of BE with distance, where c_0 is a constant, R is the heliocentric distance and α is the power law index.

Table 2 shows the BE measured above the background level from 5 to 10 R_s (columns 2 to 6, respectively). This BE

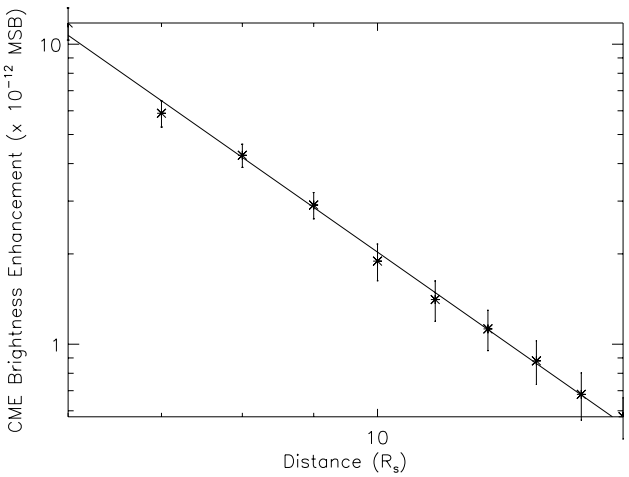

Fig. 5. Density enhancement of the CME leading edge as a function of heliocentric distance.

Table 2

CME Enhancement

date	6	7	8	9	10	α
	MSB ($\times 10^{-11}$)			MSB ($\times 10^{-12}$)		MSB/R_s
02-07-97	2.91	1.31	0.85	5.53	3.71	-3.86
04-07-97	1.61	0.69	0.49	3.26	2.10	-3.52
04-16-97	2.51	1.23	0.81	5.38	3.87	-3.57
05-12-97	0.84	0.43	0.30	1.97	1.43	-3.45
08-30-97	1.17	0.59	0.42	2.91	1.89	-3.26
09-17-97	3.49	1.75	1.22	8.31	5.78	-3.49
09-28-97	0.47	0.24	0.16	1.16	0.81	-3.53
12-06-97	3.32	1.49	0.95	6.05	4.64	-3.64
12-26-97		1.85	1.17	7.03	4.87	-3.84

is directly related to the CME density, although we do not have a calibration function to transform from brightness to electron number. However, it is possible to use this enhancement as a proxy to the relative CME density. In our CME list, the 09-17 97 CME is the brightest (highest density) with a value of 3.5 $\times 10^{-11}$ mean solar brightness (MSB) units at 6 R_s whereas the 09-28-97 CME is the weakest with 4.7 $\times 10^{-12}$ MSB at 6 R_s. The computed pawer law exponent α, for each CME is tabulated in column 7. The mean value of α is -3.6 and ranges from -3.3 to -3.9 MSB/R_s for the 08-30-97 and 02-07-97 CMEs, respectively. This exponent represents the rate of density decrease with distance. We note that this value is greater than the accepted value of $\alpha = -2$ for the ambient corona density fall off (Leblanc *et al*., 1998). This result may be reflecting a higher expansion rate of the CMEs compared with the ambient solar wind.

5. CME SPEED

CME speed is one of the frequently measured CME parameters (St. Cyr, 1999; Yashiro *et al*., 2003). The traditional method of measuring the speed is from the manual measurement of the CME height in each frame and then fitting a polynomial to the measurements. This traditional approach is somewhat subjective, so errors and discrepancies between different observers are common.

In order to systematize the speed measurement we use the information of the gaussian fit to the brightness enhancement. We were able to follow the time of the maximum (and the outer edge) of the gaussians, and since each gaussian corresponds to a fixed distance (see sec. 2), the computation of the CME speed is straightforward. This approach has two advantages: First, the speed measurements are free of fluctuations or errors due to the observer criteria (with the exception of the CPA selection). Second, we are able to perform a simple error analysis.

The disadvantage of the method is that the independent variable is the distance (we are choosing to measure the CME characteristics at 6,7,..15 R_s), and the time of maximum brightening is the dependent variable. We don't have a clear method to assign errors to the independent variable; by taking half of the minimum scale gives errors too small and assuming a Poisson distribution gives errors too large. On the other hand we are able to compute the errors in the maxima times. Then, in order to make a better error analysis, we use time-height (T-H) plots instead the traditional H-T plots.

Figure 6 shows the plot of the time of each gaussian maximum as a function of distance (in R_s). The straight-line is the first order polynomial adjusted to the points. In the example shown, the speed of the brightest part of the CME (V_{max}) is 538.4 ± 62.0 km/s.

If we know the width and peak time of the gaussians, it is possible to compute the time of the CME outer edge (OE) defined as the time of the maximum plus half of the width of each gaussian. Figure 7 shows the outer edge T-H plot, the straight-line is the first order fit to the data. In this case the OE speed (VOE) is 933.83 ± 186.67 km/s. It is interesting to note that the speed changes considerably if we use the brightness maxima or the OE times.

As seen in Figure 7 and as reflected in the large associated errors, the OE speed have large fluctuations. This is due to the TD fluctuations and may reflect real changes in the CME structure due to CME - ambient corona interactions.

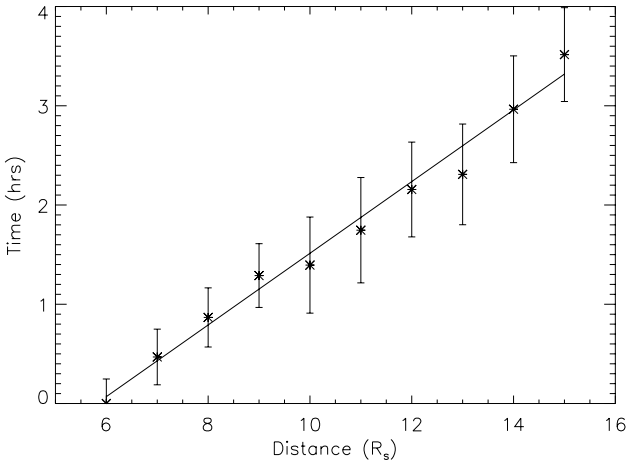

Fig. 6. Time of the brightness enhancement peak as a function of heliocentric distance. The continuous line is the first order polynomial fit to the points.

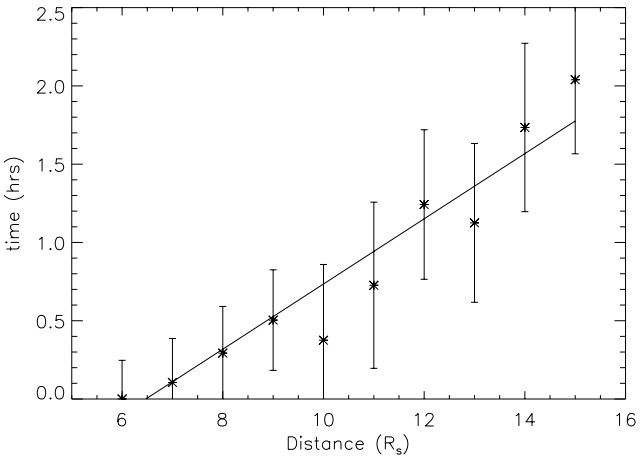

Fig. 7. T-H plot for the gaussian "outer edges" defined as the gaussian maximum plus the width (see Figures 3 and 4).

The V_{max} and V_{OE} are tabulated in the second and third columns of Table 3, respectively. Note that V_{OE} is only an approximation because we fit a gaussian (i.e. symmetrical) function to the BE which could or could not be symmetric. In order to compare the method with the traditional method, we need to compare our speeds with those from the SOHO CME catalog: the CME speed obtained by fitting a first order polynomial (V_{CSPSW}) and the CME speed computed at 20 R_s using the acceleration obtained from a second order fit (V_{20}), The speeds V_{CSPSW} and V_{20} are listed in Table 3 (columns 4 and 5).

Depending on the behavior of CME DT , V_{max} and V_{OE} can have almost the same value (when the DT does not change with time) as is the case for 02-07-97 and 04-16-97 CMEs. On the other hand, the 12-06-97 CME shows the highest difference between V_{max} and V_{OE}. This is due to the CME structure, in this case, two peaks seems to be interacting; the first one which passed at ~15: 40 at 6 R_s was a short time pulse, the second one was a longer pulse with a peak at ~18: 50 at 6 R_s. The amplitude of the second one was decreasing with the distance. At 6 R_s the second peak was higher than the first peak whereas at 10 R_s the amplitude was half of the first peak. The decaying second peak modified the computed TD in such a way that at 6 R_s the CME leading part has a long TD whereas at higher distances (> 10 R_s) the TD decrease dramatically. So the V_{max} is relatively high (956 km/s) reflecting the movement of the first peak. On the other hand, V_{OE} (434 km/s) is lower, and reflects the fact that the second peak is disappearing. As mentioned above this can be the result of the CME ambient corona or CME-CME interactions.

There are discrepancies between values obtained with this method and the C_{SPSW} values for the speed. The differences may be due to the fact that V_{CSPSW} and V_{20} were computed using C2 and C3 data and V_{20} includes the CME acceleration. However, taking into account the standard deviation, the V_{max} and/or V_{OE} of all except three CMEs (04-07-97, 09-17-97 and 09-28-97) are inside the range of V_{CSPSW} and V_{20}. This indicates a reasonable agreement. The differences may be the result of measurements of different structures at different angles and are reflecting the complexity of CMEs.

Table 3

CME speed

date	V_{max}	V_{OE}	V_{CSPSW}	V_{20}
02-07-97	634.82 (77.07)	570.66 (62.28)	490	635
04-07-97	685.10 (46.60)	1036.15 (106.59)	878	896
04-16-97	190.31 (13.42)	173.91 (11.20)	87	323
05-12-97	268.00 (53.27)	370.27 (101.69)	464	220
08-30-97	538.43 (62.06)	933.83 (186.67)	371	551
09-17-97	188.49 (16.32)	311.69 (44.63)	377	377
09-28-97	489.32 (57.63)	541.44 (70.56)	359	409
12-06-97	956.34 (321.17)	434.54 (66.31)	397	525
12-26-97	272.59 (18.20)	366.44 (32.88)	197	378

6. LIMITATIONS

Knowing of CME parameters is of fundamental importance to understand the physics of such phenomena. Even if the limitations of the present observations do not permit a precise evaluation of these parameters, approximations may be useful for both theoretical and computational models. There are limitations of the method described above. The important ones are:

- The low temporal resolution of the CME data makes it difficult to obtain a good coverage of the BE, and results in a low level of confidence in the fitting process. To minimize the problem of lack of points during the fitting process, we make an interpolation of the data points during the BE. This interpolation does not alter the data but makes the fitting process easy.

- The method can give confusing results in the case of complex (multiple peaks) or low intensity events. This problem, as well as the previous, can be solved by increasing the temporal resolution of the observations.

- Fitting a gaussian to compute the CME parameters is straightforward. This is a very good approximation when the CME is simple and has a regular peak. In the case of asymmetric or complex CMEs, a gaussian would not give the best CME parameters. To solve this problem, we are planning to make a statistical study of the shape and complexity of the CME leading part, so that select the best fitting function.

Since our primary goal is to understand the interaction of the Earth directed CMEs with the interplanetary medium, we considered a series of halo CME. In the future, we will apply this method to limb CMEs and compare the results with those of the present study. Also, we are planning to extend the method to analyze LASCO C2 data in order to obtain an extended profile of the CME parameters.

7. CONCLUSIONS

We have presented a new method to determine the CME leading edge parameters at different heliocentric distances based on the analysis of LASCO C3 data. Applying this method to a set of 9 halo CMEs observed in 1997, we found that the CME time duration near the Sun ranges from 4.9 to 12.6 hrs. with a mean duration of ~ 8 hrs. The CME transiting at different heights is seen as a brightness enhancement. Measuring this enhancement relative to the background brightness give us the possibility to obtain a proxy for the relative CME density. The maximum value observed at 6 R_s is 3.5 $\times 10^{-11}$ MSB and the CME enhancement takes all values down to 13% of this value at 6 R_s. The enhancement value falls with the distance as a power law, with the exponent in the range -3.3 to -3.9 and with a mean value of -3.6. The CME speeds have been evaluated at two points: at the brightness maximum and at the outer edge of the CME. The computation of V_{max} has higher confidence as seen by the low standard deviation values. On the other hand the V_{OE} carry the errors of the CME time duration plus the errors of the V_{max}, resulting in large standard deviation values that lower the level of confidence in the speed computation. The V_{max} are comparable with CME speeds measured by other observers.

The method of analysis has some limitations, but seems to be useful to obtain realistic values for the CME time duration needed as an input to simulation studies. It is also possible to use the brightness enhancement as a proxy for the evaluation of the relative CME density. Finally, the speed of the brightness enhancement can be computed systematically free of fluctuations due to observer differences.

AKNOWLEDGEMENTS

This research was partially suported by CONACyT grant 33321-E and DGAPA-UNAM grant 1N119402. The SOHO/LASCO data used here are produced by a consortium of the Naval Research Laboratory (USA), Max-Planck-Institut für Aeronomie (Germany)), Laboratoire d'Astronomie (France), and the University of Birmingham (UK). SOHO is a project of international cooperation between ESA and NASA.

BIBLIOGRAPHY

BRUECKNER, G. E., R. A. HOWARD, M. J. KOOMEN, C. M. KORENDYKE, D. J. MICHELS, J. D. MOSES, D. G. SOCKER, K. P. DERE, P. L. LAMY, A. LLEBARIA, M. V. BOUT, R. SCHWENN, G. M. SIMNETT, D. K. BEDFORD and C. J. EYLES, 1995. The Large Angle Spectroscopic Coronagraph (LASCO). *Sol. Phys., 162,* 357.

GONZÁLEZ-ESPARZA, A., A. LARA, A. SANTILLÁN, E. PÉREZ-TIJERINA and N. GOPALSWAMY, 2002, Numerical Study on the Acceleration of Coronal Mass Ejections in the Interplanetary Medium. *J. Geophys. Res., (in press).*

GOPALSWAMY, N., M. R. KUNDU, Y. HANAOKA, S. ENOME, J. R. LEMEN and M. AKIOKA, 1996. Yohkoh/SXT observations of a coronal mass ejection near the solar surface. *New Astronomy, 1,* 3, 207.

GOPALSWAMY, N., A. LARA, R. P. LEPPING, M. L. KAISER, D. BERDICHEVSKY and O. C. ST. CYR, 2000. Interplanetary Acceleration of Coronal Mass Ejections. *GRL, 27, 2,* 145.

GOPALSWAMY, N., A. LARA, M. L. KAISER and J.-L. BOUGERET, 2001a. Near-Sun and near-Earth manifestations of solar eruptions. *J. Geophys. Res., 106, A11,* 25261.

GOPALSWAMY, N., A. LARA, S. YASHIRO, M. L. KAISER and R. A. HOWARD, 2001b. Predicting the 1-AU arrival times of coronal mass ejections. *J. Geophys. Res., 106, A12,* 29207.

GUHATHAKURTA, M., 1989. The Large and Small Scale Density Structure in the Solar Corona. Ph.D. Thesis, University of Denver.

LEBLANC, Y., G. A. DULK and J.-L. BOUGERET, 1998. Tracing the Electron Density from the Corona to 1au. *Sol. Phys., 183,* 165.

ST. CYR, O. C., J. T. BURKEPILE, A. HUNDHAUSEN and A. R. LECINSKI, 1999. A comparison of ground-

based and spacecraft observations of coronal mass ejections from 1980-1989. *J. Geophys. Res., 104, A6,* 12493.

VAN DE HULST, H. C., 1950. The electron density of the solar corona. *Bull. Astron. Inst. Neth., 11*, 135.

VENNERSTROEM, S., 2001. Interplanetary sources of magnetic storms: A statistical study. *J. Geophys. Res.,* 106, A12, 29175.

WEBB, D. F., E. W. CLIVER, N. U. CROOKER, O. C. ST. CRY and B. J. THOMPSON, 2000. Relationship of halo coronal mass ejections, magnetic clouds, and magnetic storms. *J. Geophys. Res.,* 105 7491.

Alejandro Lara[1], Américo González-Esparza[1] and Nat Gopalswamy[2]

[1] *Instituto de Geofísica, UNAM, México D.F., 04510, México*
Email:

[2] *NASA/GSFC, Greenbelt, MD, USA*